Theor. Appl. Climatol. 61, 161–175 (1998)

Theoretical and Applied Climatology

Alaska Climate Center, Geophysical Institute, University of Alaska Fairbanks, Fairbanks, Alaska, U.S.A.

Solar Radiation Climatology of Alaska

D. Dissing and **G. Wendler**

With 11 Figures

Received July 16, 1997
Revised May 18,1998

Summary

There are only six locations in Alaska for which global radiation data of more than a year in duration are available. This is an extremely sparse coverage for a state which covers $1.5\times10^6\,km^2$ and stretches over at least three climatic zones. Cloud observations are, however, available from 18 stations. We used fractional cloud cover and cloud type data to model the global radiation and thus obtain a more complete radiation coverage for Alaska. This extended data set allowed an analysis of geographic and seasonal trends.

A simple 1-layer model based on Haurwitz's semi-empirical approach, allowing for changes in cloud type and fractional coverage, was developed. The model predicts the annual global radiation fluxes to within 2–11% of the observed values. Estimated monthly mean values gave an average accuracy within about 6% of the measurements. The estimates agree well with the observations during the first four months of the year but less so for the last four. Changing surface albedo might explain this deviation.

Previously, the 1993 National Solar Radiation Data Base (NSRDB) from the National Renewable Energy Laboratory (NREL) modeled global radiation data for 16 Alaskan stations. Although more complete and complex, the NREL model requires a larger number of input parameters, which are not available for Alaska. Hence, we believe that our model, which is based on cloud-radiation relationship and is specifically tuned to Alaskan conditions, produces better results for this region. Annual global solar radiation flux measurements are compared with results from global coverage models based on the International Satellite Cloud Climatology Project (ISCCP) data. Contour plots of seasonal and mean annual spatial distribution of global radiation for Alaska are presented and discussed in the context of their climatic and geographic settings.

1. Introduction

Any meteorological consideration for the state of Alaska has to take into account the large area it covers: from Barrow in the north (71° N) to the Tongas National Forest in the south (54° N) and from the outer Aleutian Islands (173° E) all the way to Misty Fjords National Park (130° W) – a span of 17° latitude and 57° longitude. Naturally, climatic conditions are not uniform over such a large area. There are at least three broad climatic zones in Alaska. The southern part of the state is maritime, with cool summers and relatively warm winters; the Interior is subarctic continental with relatively warm summers and cold winters, while the northern part of Alaska is arctic, with cool summers and cold winters. In addition, several physical barriers (the Brooks, Alaska, Chugach, Aleutian and Wrangell-St.Elias ranges) impact the flow patterns. Dominant synoptic-scale meteorological features which influence the Alaskan climate are the strong, semi-permanent Aleutian low and the Siberian and Arctic anticyclones. The strength of the Aleutian low varies with season; it is deeper during the winter months, at which time an anticyclone is frequently located over Central Alaska (Martyn, 1992).

Long term time series (>1 year) of global radiation are sparse for Alaska, consisting of data from only six stations. Nevertheless, global radi-

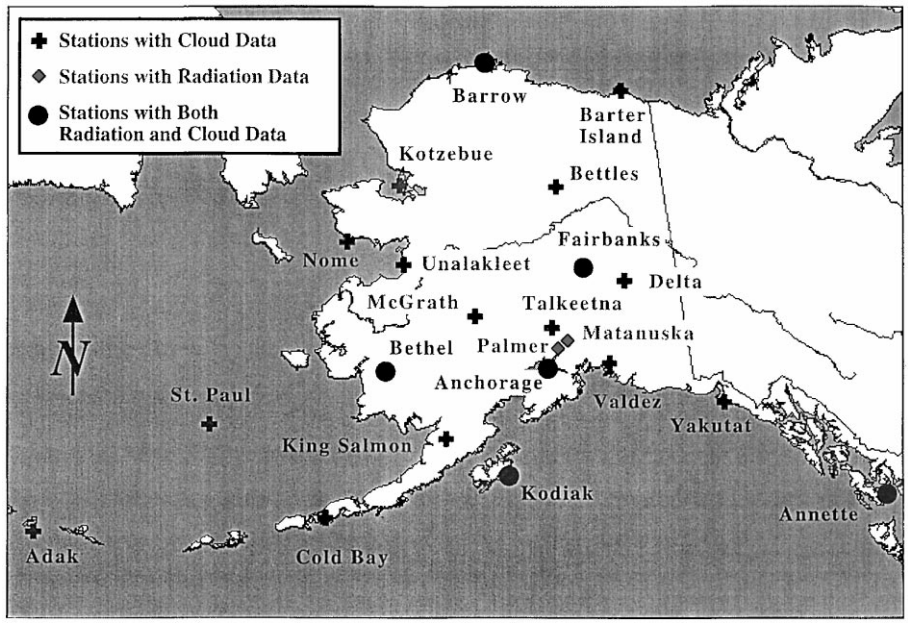

Fig. 1. Map of Alaska with the locations of stations included in the study

ation is the most widely measured radiation quantity and is therefore chosen as the base for this climatology. It is defined as the sum of the direct beam and diffuse radiation, normally measured with a pyranometer on a horizontal surface, typically in the range of 0.3–3 μm. A map with locations of the stations is shown in Fig. 1, and the years of observations are given in Fig. 2. The station in Barrow is the same NOAA CMDL site which is part of the World Climatological Research Programme (WCRP) Baseline Surface Radiation Network (BSRN). Furthermore, the Anchorage station includes data from three stations: Anchorage, Palmer and Matanuska.

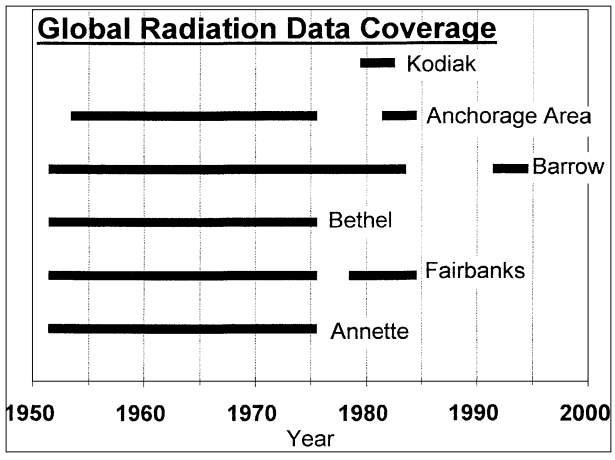

Fig. 2. Years of measurements for the included global radiation time series

Cloud observations from 18 stations located in different climatic regions of the state are available. Fractional cloud cover (tenths) and the following cloud types are used here: Cumulus (Cu), Stratocumulus (Sc), Stratus (St), Altocumulus (Ac), and Cirrostratus (Cs). The stations and years of observations used to calculate the global radiation are listed in Table 1, and their locations are shown in Fig. 1. The locations where both cloud and radiation data exist were used to tune our model to produce estimates of

Table 1. *Cloud Stations and Years Listed by Climate Region*

Region	Station	Years	Radiation data
Southern	Anchorage	1954–75	*
Coastal	Annette	1952–75	*
	Adak	1952–78	
	Cold Bay	1979–82	
	Kodiak	1980–82	*
	Valdez	1979–82	
	Yakutat	1979–82	
West Coast/	Barrow	1953–83	*
Arctic Ocean	Barter Island	1979–82	
	Bethel	1952–75	*
	King Salmon	1979–82	
	Kotzebue	1979–82	
	Nome	1979–82	
	St Paul Island	1979–82	
	Unalakleet	1969–72	
Interior	Fairbanks	1952–75	*
	McGrath	1979–82	
	Talkeetna	1979–82	

average global radiation; thus allowing us to extend the existing radiation network.

Attempts to correlate solar radiation and cloud type and amount date back to Ångström (1924). More recent papers have been published by Davies et al. (1975); Suckling and Hay (1977); Atwater and Ball (1981); and Meyers and Dale (1983). In 1993, a major effort was carried out by the National Renewable Energy Laboratory (NREL) which compiled the National Solar Radiation Data Base (NSRDB). The NSRDB is a collection of measured and modeled solar radiation data for the period 1961–1990 for the United States. The data base output is global, diffuse and direct solar beam radiation. When measured data were available, these values were presented in the data base, otherwise a model was employed to produce estimated values. The model estimates are based, with a few modifications, on cloudless sky direct normal transmittance algorithms as given by the models of Bird and Hulstrom (1981) and Iqbal's parameterization model C (Iqbal, 1983). Measured radiation data constitute less than 7% of the NSRDB. For Alaska, this number is even smaller. One (Fairbanks) of the 17 stations for the state is measured while the other 16 are modeled. The part of the NREL model which covers Alaska is thus tuned on a single data point. Hence, our goal was to construct a model tuned to the varying radiation-cloudiness relationships within Alaska. The International Satellite Cloud Climatology Project (ISCCP) provide global cloud distribution data. Several projects make use of the cloud data as input in models predicting solar radiation fluxes. Results from two of these studies, Rossow and Zhang (1995) and Darnell et al. (1992), are included for comparison.

2. Model Setup and Description

The purpose of our model is to predict global radiation for locations in Alaska (often remote), where no previous long-term radiation measurements were carried out. For these areas, limited meteorological data are available. A complete radiative transfer model, which requires extensive amounts of input parameters, would not be appropriately supported. In addition, the longest available radiation data series for Alaska (Annette Island, Matanuska, Bethel, Fairbanks and Barrow) have known problems (Wise, 1979). Hence, we chose a relatively simple model, for which the input data were available. It is a modified version of Haurwitz's semi-empirical equation (Haurwitz, 1945), which depends only on cloud parameters and optical air mass:

$$H = \left(\frac{a}{m}\right) e^{-bm}$$

where H = global radiation

m = optical air mass (secant to the solar zenith angle)

a,b = constants (determined by least squares method)

The reason for applying this exponential expression is the assumption that solar radiation received on a horizontal surface can be approximated as an exponential function of air mass. We used this expression but modified it to incorporate the effects of changing fractional cloud cover and cloud type.

The global radiation data for each of the five stations were treated separately, and sorted into groups by intervals of optical air mass at solar noon, fractional cloud cover (0; 1–3; 4–7; 8–9; 10 tenths coverage) and cloud type (Cu, Sc, St, Ac, Cs). These cloud types were chosen as they were the most frequently observed. The constants a and b were then determined for each sorted group. Using the method of least squares and simple iteration, the constants a and b for each station could be determined allowing us to calculate the incoming radiation for each cloud type. For each fractional cloud cover interval a ratio is taken between the clear sky case a- and b-values (a_0; b_0) and the cloudy case a- and b-values (a_c; b_c). Assuming a linear change in the a_0/a_c and b_0/b_c ratios with cloud cover, the ratios are modeled as: $a_0/a_c = z + x^{*}cc$, where cc is the fractional cloud cover. The same procedure is followed for b_0/b_c. Using the two linear expressions thus obtained, we can now estimate the ratios for any given fractional cloud coverage. Substituting these linear expressions back into the original equation yield the expression for the cloudy sky case.

We then have the general expression:

$$H_{ct} = \left(\frac{a_0(z + x{*}cc)^{-1}}{m}\right) e^{-(b_0(z' + x'{*}cc)^{-1})m}$$

where ct = cloud type

cc = fractional cloud cover

If the cloudiness is zero ($cc = 0$), this expression simplifies to:

$$H_0 = \left(\frac{a_0}{m}\right) e^{-b_0 m}$$

This allowed the calculation of the average global radiation for each station for each day of the year. However, for the two stations, Barrow and Bethel, the yearly course in global radiation is very skewed. To obtain a better fit for these two data series, we employ two separate sets of functions, used for the periods of January–June and July–December. An explanation for why this was necessary might be that the above derived equation does not consider the influence of surface reflectivity (and with it multiple reflection): these effects are most pronounced in areas with long lasting snow cover and little vegetation.

In general, the modified Haurwitz model showed transmittance to increase with decreasing air mass and decreasing cloudiness. The cloud type had greatest influence on the transmissivity at lower air masses and at higher fractional cloud coverage. The lowest level cloud layer was the least transmittant, the middle layer intermediate, and highest levels transmitted the most energy. This trend is in agreement with earlier studies (Haurwitz, 1948; Vowinckel and Orvig, 1962; Atwater and Ball, 1981; Kasten and Czeplak, 1980), which also suggest that the often vertically extensive cumuliform clouds are the least transmittant. However, the Alaska data do not support this latter finding. Probably this is due to the fact that the Alaskan cumulus clouds are of smaller vertical extent than those observed at lower latitudes. We found stratus clouds to transmit, on the average, the least amount of solar energy.

3. Results

In Fig. 3, the modeled and measured global radiation are presented for Fairbanks. All lines represent daily averages for the observational period and an 11-day moving average filter has been applied to the data to suppress noise. The uncertainty of the model output is estimated as $\pm$ 1 standard error (S_e), which is defined as the standard deviation of the estimate of the mean (Davis, 1986). In general the agreement is good; however, the model slightly underestimates the mean annual value for Fairbanks. Further, there is an annual course in the difference between observed and modeled values (see Fig. 3b). For all five stations, the model underestimates the spring values, and overestimates the fall values. This is most likely caused by changing surface albedo, which would give higher observed values in spring due to multiple reflection between the highly reflective snow covered surface and the clouds/atmosphere. However, this is not considered in our model. A second explanation might be an annual variation in the optical depth for any of the five selected cloud types, causing varying quantities of global solar radiation to be transmitted at different seasons although the same cloud types were present.

For all five stations, the model predicts the mean annual flux within 2–11% of the observed values. Examination of the individual fits show that the largest errors occur when estimating St or Cs cloudy days. Again, this might be caused by an annual variation in optical depth for these two cloud types. However, data quality is also an important issue when working with historical data. The radiation data used as the base of this study is the 1952–1975 NOAA data set, for which inaccuracies are known to exist, but have not been well quantified. Wise (1979) expressed his concern that the stated 2% uncertainty about the measurements was often exceeded. The uncertainties of the measurements have been set at 5–20% in this paper, based on subjective corrections applied by Wise. Since these uncertainties are of the same order as the differences between the observations and the model estimates, no refinements of the model appears worthwhile without new, more accurate data sets.

Figure 4 shows scatter plots of the observed versus the modeled global radiation for the five stations at Annette Island, Matanuska, Bethel, Fairbanks and Barrow. The straight line represents the case in which the observed and modeled data are identical, and the triangles show the modeled data points. The correlation coefficient (r), is shown for the individual plots, and it can be seen to exceed 0.97 for all stations. The data points do not describe a straight line. The model appears to underestimate the very high values, but overestimate the values in the mid-range. These patterns are especially pronounced for

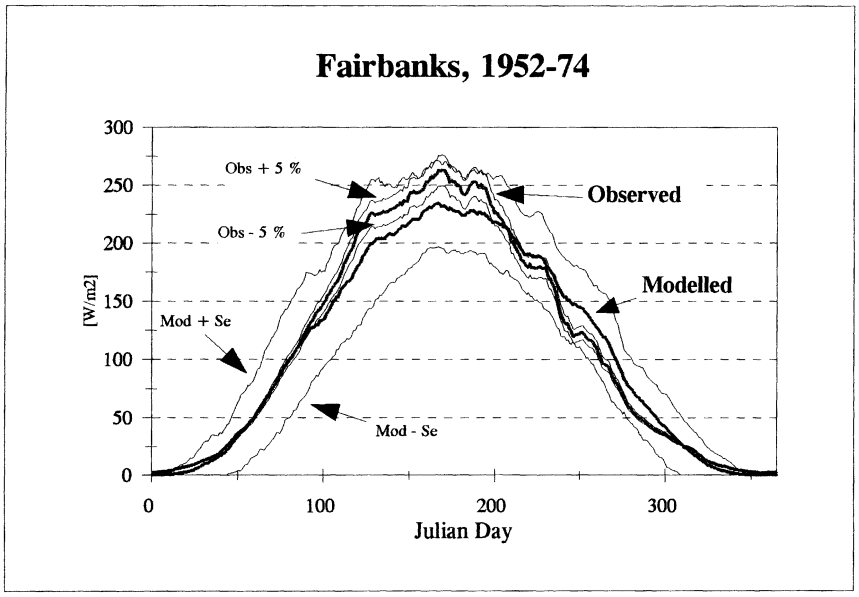

a.

Yearly averages :

Observed	total	40770.5 W/m2
	avg/day	111.7 W/m2
Modelled	total	39571.5 W/m2
	avg/day	108.415 W/m2

% error in annual estimate : 2.5

Avg error in daily estimate : 12.6 W/m2

b.

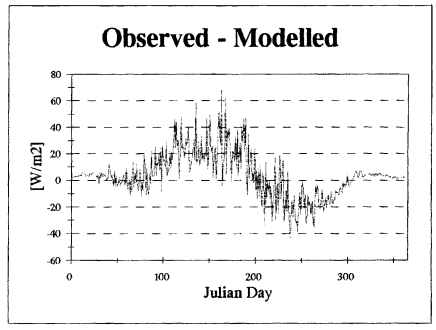

Fig. 3. Modeled and observed mean annual global radiation (bold line) at Fairbanks station in the Interior. Uncertainties (Wise's corrections): Observed values ± 5%. Error about the estimate: Estimate ± $1\,S_e$ (standard deviation). Uncertainties are plotted in thin lines. b Actual differences (observed – modeled values) in Wm^{-2}

Annette, Fairbanks and Matanuska, and must be due to a bias in our model, introduced by the assumption of linear decrease of the exponent in our expression for global radiation with increased fractional cloud cover.

Using the five derived sets of equations established from the stations where radiation was previously measured, we were able to extend our radiation coverage to places where only cloud observations were available. A base station was chosen for each individual case by similarities in climatic region and vegetation type. Table 2 shows the modeled mean monthly global radiation values for the 12 Alaskan cloud stations.

The quality of these calculations is, of course, dependent on the quality of the model and the cloud observations. Visual cloud observations are subjective, and have often been a topic of discussion (Curry et al., 1996; Schweiger and Key, 1992). However, the main problems we encountered were inconsistent reporting hours throughout the state, and use of identical codes for missing data and measured quantities. In general, however, the data quality does appear to be satisfactory. Figure 5 is a comparison between the visually determined fractional cloud cover (Barrow and Barter Island) and data based on ceilometer measurements at Barrow. The two data series are not completely compatible, since they report the cloud cover based on different fields of view. The ceilometer measures the cloudiness at zenith, and is not consistently reporting high cirrus, whereas the surface observer evaluates the mean cloudiness based on the whole sky view. A systematic difference between the two observation types is thus to be expected. Furthermore, the data series shown in Fig. 5 represent different time periods. Nevertheless, a similar mean annual course of cloudiness is observed in all the data sets (Fig. 5), giving support to the surface observations used in our calculations. Schweiger and Key (1992) discuss similarities and differences between the surface-based cloud reports and two satellite

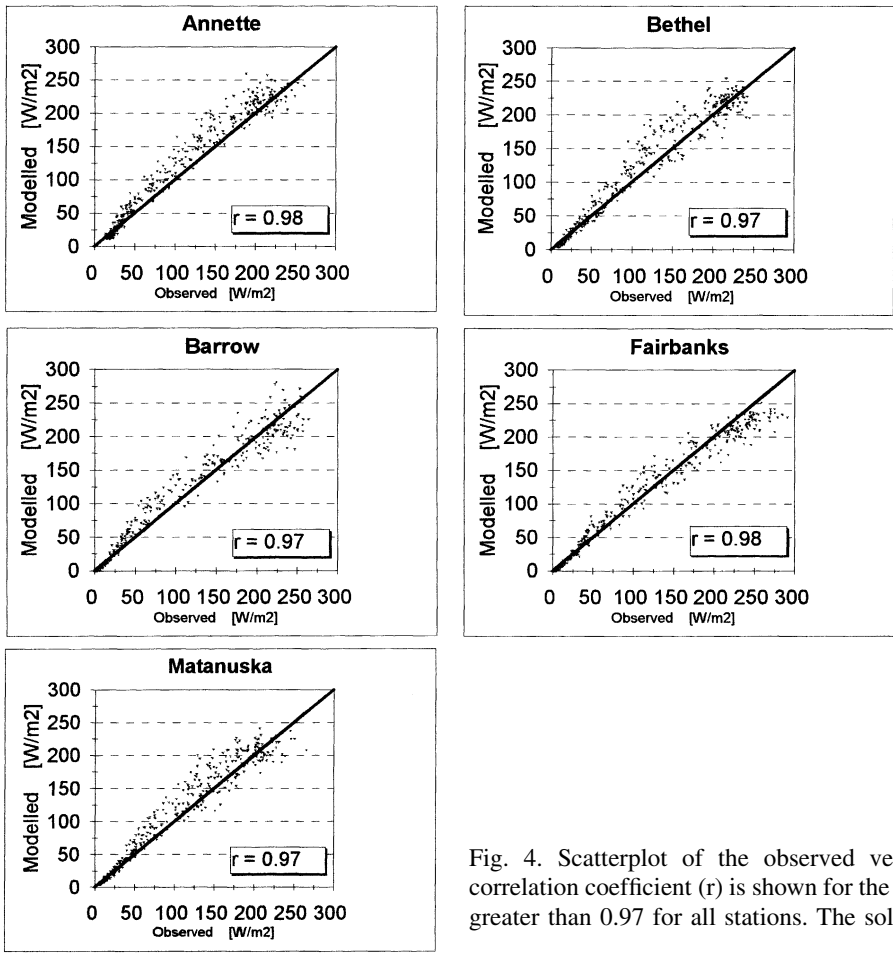

Fig. 4. Scatterplot of the observed versus modeled global radiation. The correlation coefficient (r) is shown for the individual plots, and can be seen to be greater than 0.97 for all stations. The solid line is the 1:1 line

Table 2. *Estimated Mean Monthly Global Radiation by Haurwitz's Model*

	Adak	Barter Island	Cold Bay	King Salmon	Kotzebue	McGrath	Nome	St Paul Island	Talkeetna	Unalakleet	Valdez	Yakutat
January	46.11	0.04	32.40	19.92	0.75	8.57	3.02	23.15	9.16	4.14	12.83	6.85
Feb	85.05	24.95	75.27	66.54	19.85	49.70	35.85	67.44	44.94	35.06	44.97	35.95
March	141.00	90.71	124.85	125.19	81.08	103.72	98.36	124.39	100.44	99.23	99.97	82.19
April	191.87	168.32	182.46	186.35	169.29	168.99	189.97	187.25	175.42	172.70	166.63	145.67
May	222.34	209.97	213.36	209.50	225.49	218.61	215.94	222.22	206.28	215.75	186.58	177.76
June	235.14	242.36	226.03	227.47	285.55	221.24	236.39	229.85	223.46	225.30	205.34	201.72
July	198.27	167.59	188.84	201.77	187.50	204.09	194.41	202.27	216.81	187.35	193.67	192.24
Aug	177.75	124.93	169.77	172.17	141.63	173.47	162.99	177.72	183.29	154.98	178.51	159.17
Sept	141.18	48.30	134.30	127.06	95.16	125.04	100.63	134.30	125.58	108.30	123.74	104.28
Oct	94.05	13.20	82.21	74.02	33.96	61.54	48.31	76.14	63.12	45.68	64.55	45.67
Nov	51.22	0.05	38.48	28.78	3.32	15.84	7.27	27.28	20.81	9.01	22.42	12.02
Dec	30.24	–	21.21	11.32	0.00	2.80	0.27	12.92	3.57	0.43	5.76	2.64
Year	49178.23	31036.85	44751.09	43826.63	37889.97	40467.12	39048.75	40561.56	41280.21	38250.51	39629.76	40626.22
avg/year	134.73	85.03	122.61	120.07	103.81	110.87	106.98	111.13	113.10	104.80	108.57	111.30

cloud data sets; the ISCCP and the Nimbus-7 Global cloud Climatology. Not only are the data sets based on different viewing geometry; they also use separate definitions for the high, middle and low cloud levels. These discrepancies make comparisons between the datasets nontrivial, and the satellite derived cloud data are thus not included in this climatology. For an in-depth discussion on this issue, we refer to Schweiger and Key (1992). In this paper, Schweiger and

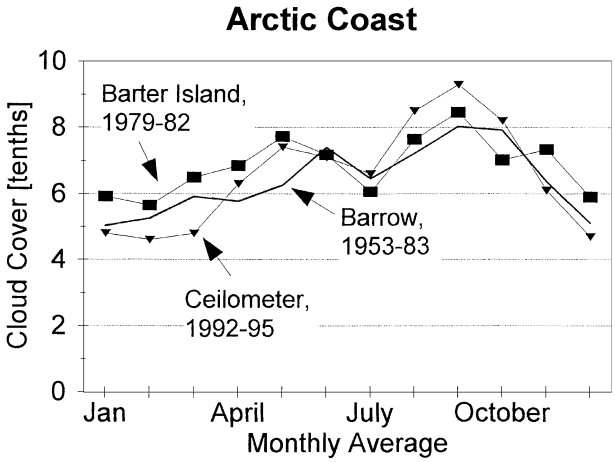

Fig. 5. Comparison between the visually determined fractional cloud cover (Barrow and Barter Island) and estimated cloud coverage based on ceilometer measurements from Barow. Note that despite the different lengths of the time series, the lines convey similar trends in the annual course

mately 5° latitude apart in the north – south direction is shown in Table 3. St/Sc dominate (around 60%) at the coastal stations (Adak, Annette, and Barrow), while they are less frequent at Anchorage and Fairbanks. Hence, low level clouds are not only dominant at the Arctic coast, but also for stations in western Alaska. In interior Alaska, St clouds rarely exceed 10%. Warren et al. (1985) conducted global cloud studies and found low-level St cloudiness to increase polewards, while Cu clouds were reported to decrease with increased latitude. Although Table 3 shows that Cu clouds do occur more frequently in South Alaska than they do at the Arctic Coast, the maximum occurrence of Cu is found in interior Alaska during the summer months. Hence, no consistent trends are indicated in the Alaskan data.

Another interesting observation is the seasonal and geographic occurrence of Cu clouds. Cu

Table 3. *Percentage Frequencies of Selected Cloud Types for 5 Stations*

Station	Latitude	Month	Cumulus	Stratus	Strato-cumulus	Avg Cumulus	Avg St/Sc
Adak	51°53 N	Jan	21	6	60	20	66
		April	28	6	53		
		July	6	18	56		
		Oct	24	3	60		
Annette	55°02 N	Jan	2	3	65	8	62
		April	13	1	54		
		July	12	7	51		
		Oct	6	3	63		
Anchorage	61°10 N	Jan	1	16	36	14	44
		April	17	3	35		
		July	33	2	32		
		Oct	3	9	42		
Fairbanks	64°49N	Jan	0	5	30	16	33
		April	14	1	32		
		July	47	2	18		
		Oct	1	6	37		
Barrow	71°18N	Jan	0	22	28	2	58
		April	1	30	22		
		July	5	36	23		
		Oct	0	34	36		

Key find the satellite fractional cloud coverage to be 5–35% less than the surface-based observations, and conclude that none of the examined cloud climatologies can be assumed the more correct version.

The average frequency in occurrences of St, Sc, and Cu for five stations, spaced approxi-

clouds form as a result of either convection or frontogenesis, and are mostly seen during the summer months throughout Alaska. Most stations have none reported during winter. Three stations display the exact opposite pattern: Adak, Cold Bay, and St Paul Island. At these stations, Cu constitutes 15–40% of the total reported

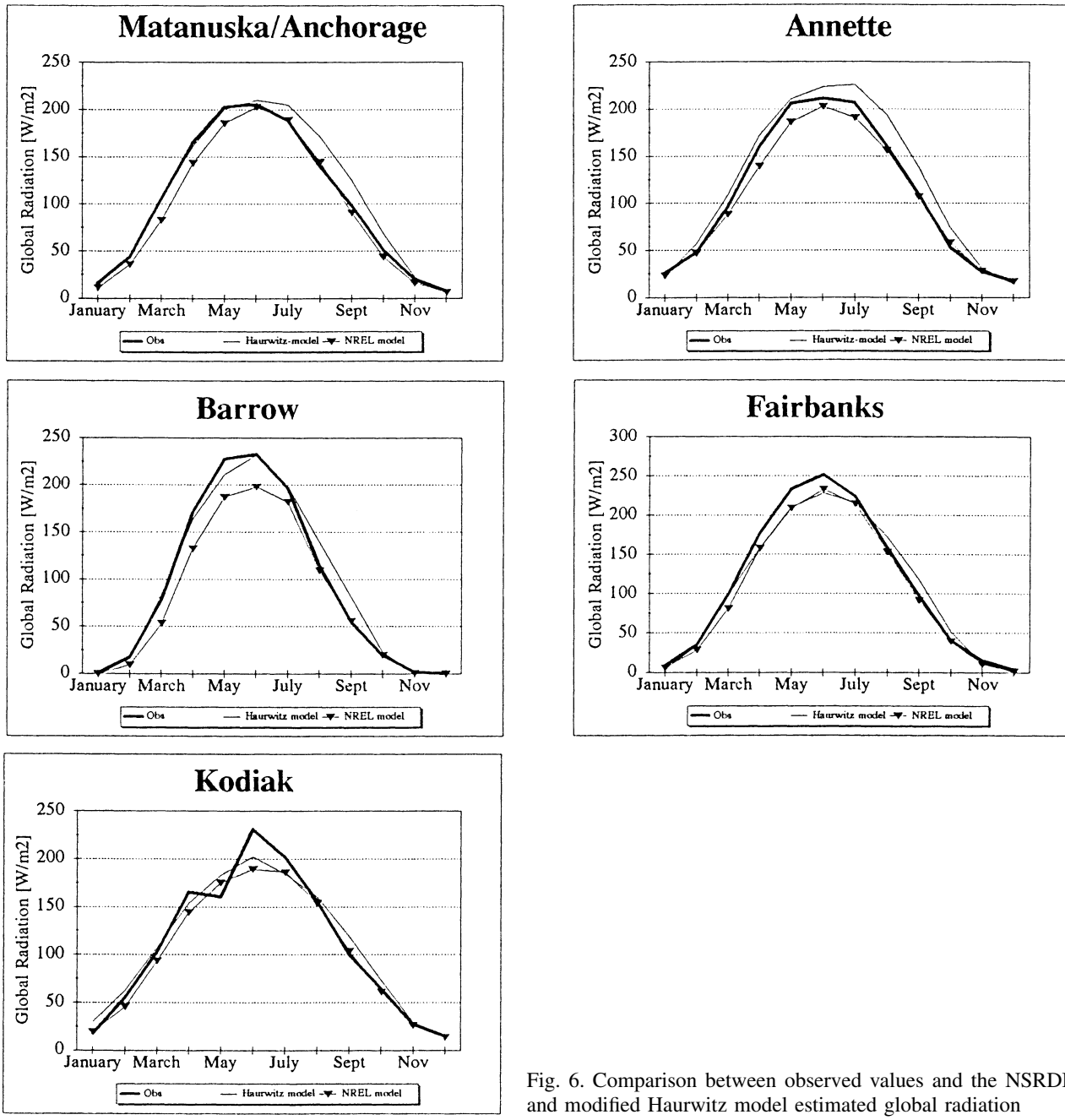

Fig. 6. Comparison between observed values and the NSRDB and modified Haurwitz model estimated global radiation

clouds all year, except for the summer months, where the frequencies suddenly drop to less than 6%. Here the Cu clouds are predominantly formed by frontogenesis, and can be explained by the seasonal summer weakening of the Aleutian low.

In general, the summer fractional cloud cover is more extensive than the winter coverage for most stations of Alaska. Stratocumulus is the most occurring cloud type in Alaska. At most stations Sc accounts for 20–25% of the reported clouds year round. This is in agreement with the findings by Warren et al. (1985). Middle level clouds (Ac and As) occur more frequently than Cirriform clouds, though less often than the low altitude clouds. Ac is observed more commonly than As. Few mid-level clouds are reported along the southern coast of Alaska. At the Arctic

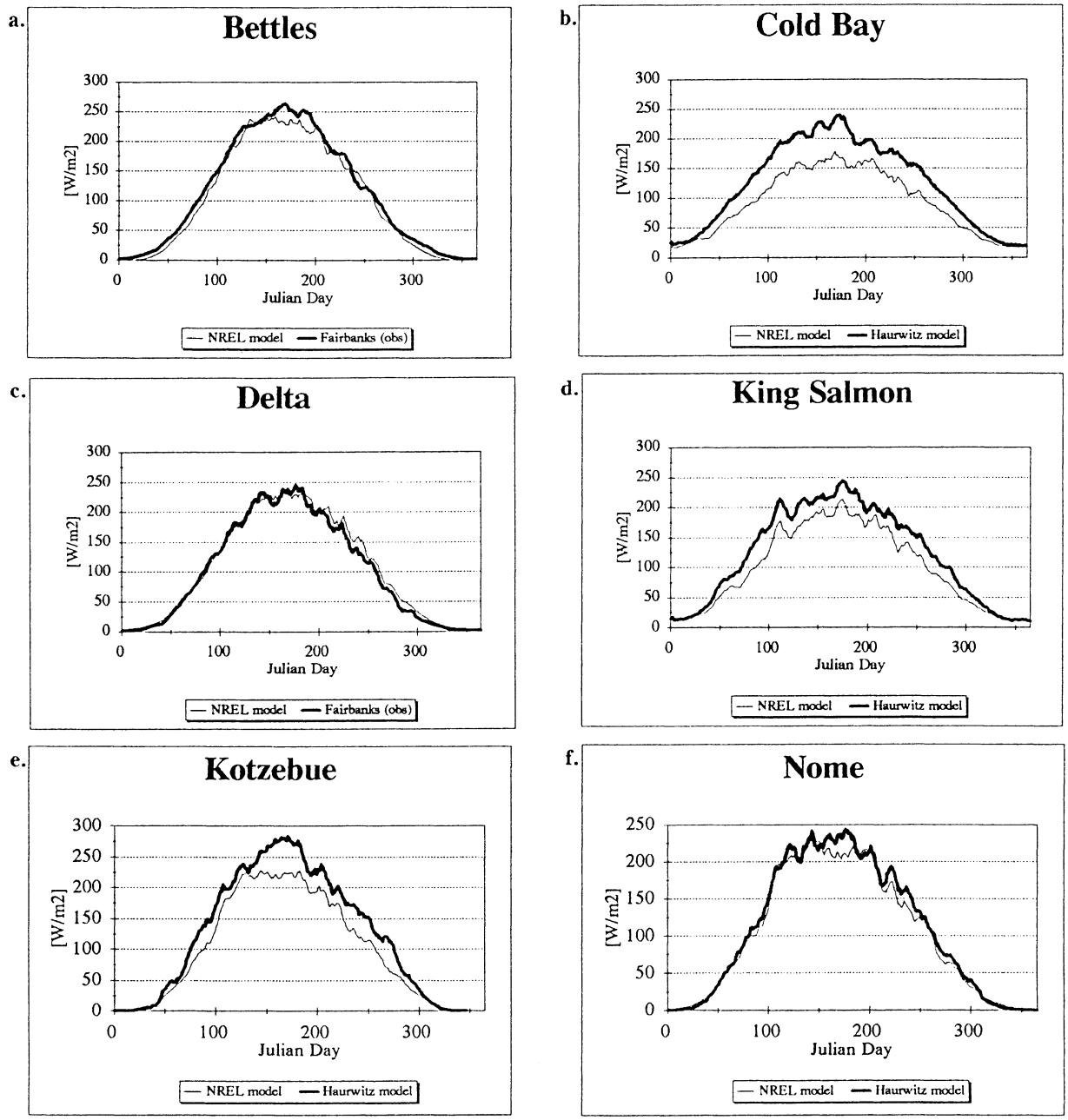

Fig. 7 (a–l). Comparison between the NSRDB (NREL model) and the modified Haurwitz model estimated global radiation values. Where model data from only one of the models exist, the nearest base station is used as a reference. All lines are 11 point moving averages

coast, the Interior, and along some of the Bering Sea coast they are present all year with a 10–25% occurrence frequency. Cirriform clouds are mostly reported during winter and spring, and then primarily in the form of Cs. Cirrus clouds are reported less often, and cirrocumulus almost never. This is in agreement with Huschke (1969) in his study of Arctic cloud statistics. He found mid-level clouds to have a similar frequency throughout the year, and high-level cloudiness to decrease during summer. It is important to notice that an extensive low cloud deck will restrict the observer's field of view and might cause these low numbers of reported middle and upper level clouds. Thus in effect, we might not actually observe a

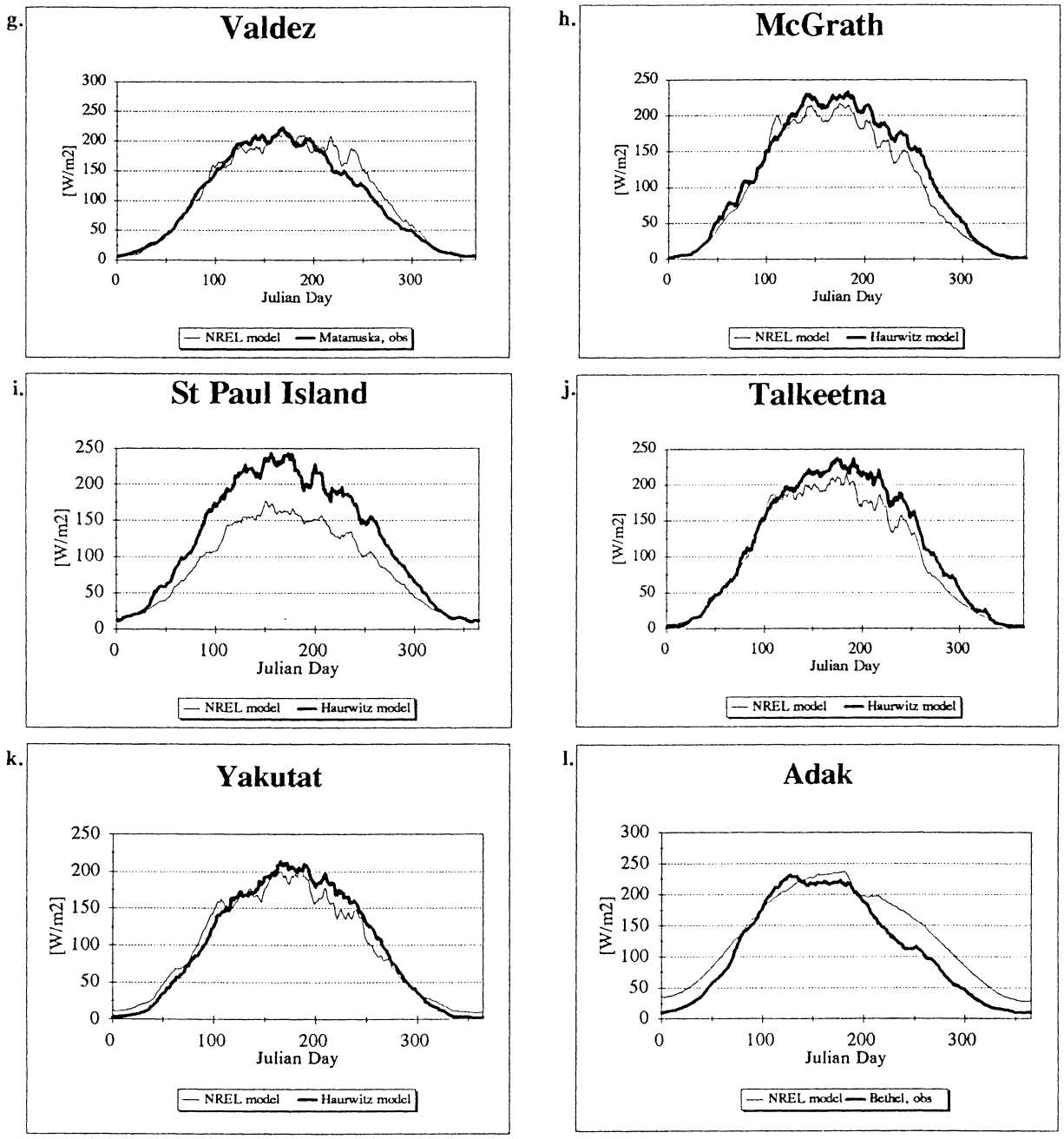

Fig. 7 (*continued*)

lack of middle clouds for the more exposed stations, but are simply prevented from quantifying them.

In Fig. 6 the annual course of the observed global radiation for the five stations, and the output derived from the modified Haurwitz model are presented. Further, the NREL model output was added to the figure. In general, the two models give quite similar output. Our model overestimate the data for fall, while the NREL model underestimate the data for spring. This is especially pronounced for Matanuska/Anchorage. In general our model does somewhat better, especially in the Arctic (see Barrow). Note further that the uneven observed annual course for Kodiak was caused by the short observational period.

Figure 7 (a–l) shows modeled global radiation for the stations where no previous measurements were conducted. Whenever possible, both the

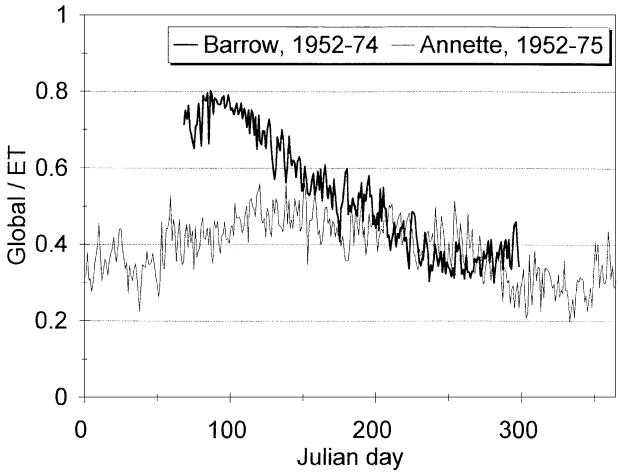

Fig. 8. Clearness Indices for the stations at Annette Island (Southeast Alaska) and Barrow (Arctic Coast). Remark the large difference between the two time series in the spring. The effect is due to the annual course in the fractional cloud cover and to multiple reflections

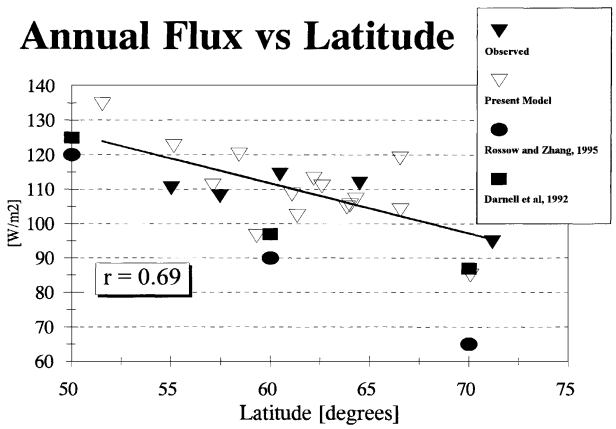

Fig. 9. Annual flux versus latitude. Observed and modeled data from this study are compared to data derived from the ISCCP cloud data by Rossow and Zhang (1995) and Darnell et al. (1992). The solid line represents the best straight line fit through the data included in the present paper with a correlation coefficient of 0.69

NREL and the Haurwitz model estimates are shown. In the cases of Bettles (a), Delta (c) and Adak (k), an estimate only exist from one of the models, and is thus shown with the nearest base station as a reference. With the exceptions of Cold Bay, St Paul Island, and, to a lesser extend, King Salmon, the values from the two models are in remarkable agreement. Often they can be observed to predict the same local maxima and minima in the time series. Such short time variations must be due to variations in the cloud cover, as this is the only short frequency input parameters in the Haurwitz model. The large deviations between the two models for Cold Bay, St Paul island, and King Salmon may be caused by the fact that these stations are far from Fairbanks and fall in a different climatic zone. Since the Fairbanks radiation measurements represent the only base from which the NREL model is fit to Alaskan conditions, these stations are expected to have the greatest associated errors. We believe that our data, which in this region is based on the cloud-radiation relationships for Bethel, are superior. However, only future measurements will help to verify this.

All stations in Alaska show that more incoming solar radiation is transmitted through the atmosphere in the spring than in the fall for identical solar elevation angles. If we consider the annual course in the fractional cloud coverage data for the respective stations, all stations show higher values in fall than in spring, making it a reasonable explanation that this could be a primary reason for the observed transmission effect. However, even for any specific cloud amount and identical solar elevation, the spring values are higher. A secondary effect, multiple reflection between the highly reflective snow cover and the clouds, enhances the radiation values (Wendler and Eaton, 1990; Iqbal, 1983; Curry et al., 1996). Studies have shown that models can underestimate incoming surface shortwave radiation substantially if the effects of multiple reflections are disregarded (Curry et al., 1996). This phenomenon is much more pronounced in the Arctic, where a very high surface albedo is observed during spring than in southern Alaska. Figure 8 presents the clearness indexes of the two extreme stations at Barrow and Annette. In addition to a shorter snow season at Annette, its location in dense, temperate rainforest vegetation causes a much less severe increase in surface albedo due to snow cover, even when snow is present. Hence, the effects of multiple reflection are not recorded for the same extended time period, nor as severely, at Annette as they are in Barrow. In addition, the variation in the annual course of the fractional cloud cover is very small in Annette. Here the primary influence on the transmissivity is the pathlength through the

atmosphere. Comparing Annette and Barrow with other Alaskan station's clearness indexes reveal that only Bethel has the same large difference between spring and fall as does Barrow. This supports the above hypothesis, since Bethel, likewise, is situated in a low vegetation zone, and therefore is expected to undergo similar surface albedo changes as Barrow. Adak too, has no tall vegetation. However, this is an island located further south than any other station considered in this study, and it has in addition a maritime climate with essentially no continental influence. Snow therefore does not have any major influence on the mean surface albedo. The clearness index at Adak shows a higher value for spring than for fall, but the amplitude of the variation is very small.

Sea ice is another important factor enhancing multiple reflections for coastal ice-bound stations. The Arctic Ocean and Bering Sea feature extensive sea ice covers for parts of the year, and are therefore much colder than the North Pacific Ocean (Martyn, 1992). Multiple reflection, enhanced by sea ice and the high albedo snow surface, together with the annual course of the fractional cloudiness, make the maximum in global radiation occur early (May) for Barrow and Barter Island. Other Alaskan stations observe it in late June, which is to be expected from the annual variations of the solar elevation angle.

Figure 9 shows the annual global radiation fluxes as a function of latitude. Both the measured and the modeled data from this study are included. The best linear regression fit is shown. For comparison, two other datasets, both based on the ISCCP cloud data are added. Rossow and Zhang (1995) calculated shortwave and longwave fluxes using the Goddard Institute for Space Studies GCM. The ISCCP data were supplemented with TIROS Operational Vertical Sounder (TOVS) and NOAA weekly snow/ice cover data. Output fluxes were calculated for the mid-seasonal months of January, April, July and October for the 4 year period from April 1985 to January 1989. Darnell et al. (1992) used a similar approach to compute shortwave, longwave and net radiation fluxes based on ISCCP and Earth Radiation Budget Experiment (ERBE) data. However, only July/October 1983 and January/April 1984 were included in this study. In general the two ISCCP-derived datasets show lower values than our modeled and the observed values. This is very interesting, especially following that the ISCCP cloudiness data in general were found to be 5–35% less than the surface-based reports (Schweiger and Key, 1992). Maybe the algorithms used for the global-scale studies do not incorporate effects like multiple reflections (as mentioned earlier) and this could cause the underestimates.

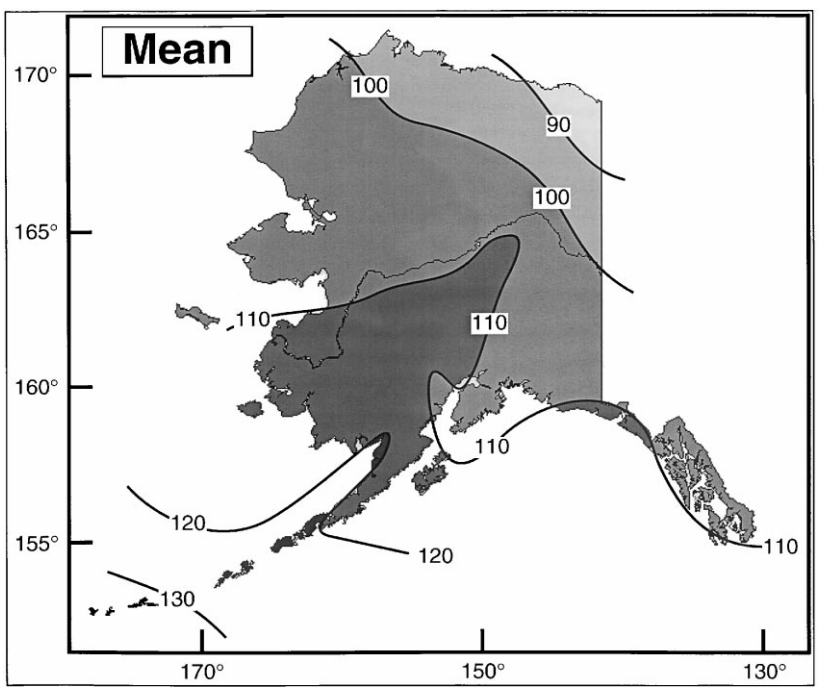

Fig. 10. Contour plot of the spatial distribution of the mean annual global radiation for Alaska. The map is based on both modeled and measured values. Latitude can be seen to have substantial influence on the annual distribution

4. Contour Plots

The average seasonal and annual spatial distribution of global radiation is shown in Figs. 10 and 11. The data base for these graphs are both measurements and modeled (modified Haurwitz model) data. Model estimates from two stations (Delta and Bettles), not included in our model study, were added from the NSRDB. The four seasonal values are calculated by averaging mean monthly values for spring (March–May), summer (June–August), fall (September–November), and winter (December–February). Over the ocean surfaces the lines were extrapolated, since no ocean stations are available. Hence, these contour lines does not take continental effects into account.

Only for winter and fall can the expected strong N–S gradient in the incoming solar radiation be observed. The summer and spring plots are more complicated. The spring plot shows a maximum at Adak station in the outer Aleutians and high values at Bethel and along the west coast. The lowest values occur at the North Pacific coast in Southeast Alaska and Kodiak Island. However, Bethel displays very low summer values which are caused by the high fractional cloud cover, higher than the surrounding stations of King Salmon, McGrath and St.Paul Island. Similarly, the North Pacific experiences a high

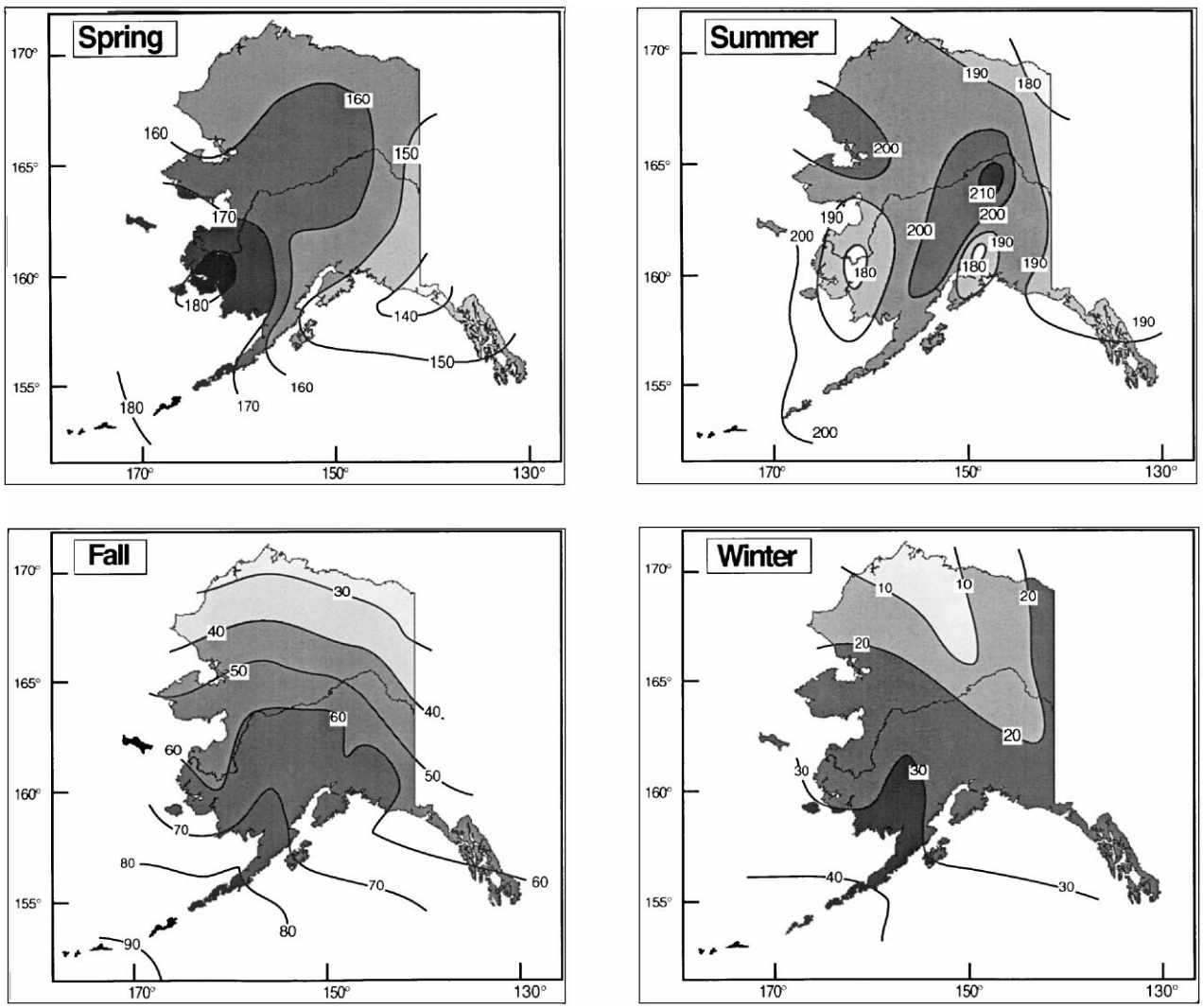

Fig. 11 (a–d). Seasonal contour plots of the spatial distribution of the global radiation for Alaska. The maps are based on both modeled and measured values. Again, latitude, but also the annual course in the fractional cloud cover strongly influences the observed pattern

fractional cloud coverage and thus low radiation values in summer. The radiation maximum in summer is received at the Interior stations; the values north of the Arctic Circle are lower due to the higher amount of cloudiness despite the 24 hours of sunlight.

The maximum annual values are found at Adak and in a zone propagating towards the Interior. Minima occur at the Arctic Coast due to the 24 hour darkness in winter and the high fractional cloud cover especially in summer. In general, latitude and the annual course in the fractional cloud cover seem to be the determining factors. For example, although the fractional cloud cover is high year-round at Adak, its southern location still causes the station to have the highest mean annual flux in Alaska.

5. Summary

Haurwitz semi-empirical model from 1945 was modified to calculate solar radiation from fractional cloud cover and cloud type. The model provided global radiation estimates within a range of 2–11% of the observed annual values and about 6% of the mean monthly values. An average deviation between the observed and modeled daily values is found to be 14.2 W/m^2. The modified Haurwitz model has uncertainties associated with it, due mostly to a large variance in the data set, and to problems with the assumptions that went into the model. Despite earlier voiced concern about the quality of the visually determined ground based cloud reports, a comparison with estimated data based on measured ceilometer data shows good agreement. In summary, the following observations about the seasonal and geographical trends in cloudiness and global radiation data have been found.

- Higher amounts of fractional cloud cover occur in the summer than in winter half of the year for most stations. Sc is the most occurring cloud type. Cirriform clouds are most abundant in winter – maybe an effect of a less extensive lower level cloud cover in winter, which would prevent the higher level clouds from being quantified. Cu clouds are mostly observed during summer and are essentially absent during winter. Adak, Cold Bay and St. Paul Island display an exact opposite pattern, which could possibly be explained by the seasonal summer weakening of the Aleutian cyclonic system.
- Higher clearness indices occur in spring than in fall for all stations. This is primarily due to the fact that the fractional cloud cover is higher in fall than in spring. A secondary effect, strongly enhanced at places where the length of the snow season and the surface albedo allow it, is multiple reflections between the highly reflective snow surface and the clouds (atmosphere).
- Contour plots of seasonal and mean annual spatial distribution of global radiation for Alaska reveal a strong influence of latitude and the annual course in the fractional cloud cover on the incoming solar radiation patterns. Annual fluxes appear higher than portrayed in global-scale solar radiation studies based on ISCCP data.
- The highest annual values are found at Adak Island in the outer Aleutian chain, which is the southernmost station included in this study. The lowest values are found at the Arctic coast due to the 24 hours of darkness during the winter months. In general, the Interior of Alaska has more incoming solar radiation than the coastal areas, except for the fall and winter months, where stronger N-S gradients exist.

6. Conclusive Remarks

Predictions from GCMs showing large changes in the future arctic/subarctic climate have brought a focus to this region that it has not earlier received. As mentioned earlier, few data exist, and more is definitely needed in order to understand the complex processes guarding the climate in the Arctic. Hopefully, ongoing studies such as the Mackenzie River GEWEX Study (MAGS), the Atmospheric Radiation Measurement (ARM) and the Surface Heat Budget of the Arctic Ocean (SHEBA) will provide a better understanding and more high quality data for the Arctic. Ideas for further research on the topic of this paper include filtering out some of the large uncertainties associated with the historical global radiation dataset and further investigating the appropriateness of the exponential base expression and the linearly decreasing exponent approach. Additionally, supplementing the sur-

face cloud reports with for example ISCCP data would allow for less uncertainty and better coverage in the cloud data.

Acknowledgements

We are thankful to W. Cantrell, J. Curtis, B. Moore, J. Simmons, W. Stringer, B. Watkins, and G. Weller for their helpful suggestions which improved this paper. The study was funded by the Alaskan Climate Research Center, State of Alaska funds, which we would like to acknowledge.

References

Ångström, A., 1924: Solar and terrestrial radiation. *Quart. J. Roy. Meteor. Soc.*, **50**, 121–126.

Atwater, M. A., Ball, J. T., 1981: A surface solar radiation model for cloudy atmospheres. *Mon. Wea. Rev.,* **109**, 878–888.

Becker, R., Leslie, L. D., 1983: Solar radiation assessment for Anchorage, Alaska. Arctic Environmental Information and Data Center, University of Alaska. Report for U. S. Department of Energy. 34 pp.

Bird, R. E., Hulstrom, R. L., 1981: A Simplified Clear Sky Model for Direct and Diffuse insolation on Horizontal Surfaces. Solar Energy Research Institute, SERI/TR-642–761.

Curry, J. A., Rossow, W. B., Randall, D., Schramm, J. L., 1996: Overview of arctic cloud and radiation characteristics. *J. Climate,* **9**/8, 1731–64.

Darnell, W. L., Staylor, W. F., Gupta, S. K., Ritchey, N. A., Wilber, A. C., 1992: Seasonal variation of surface radiation budget derived from international satellite cloud climatology project C1 data. *J. Geophys. Res.,* **97**/D14, 15,741–15,760.

Davies, J. A., Schertzer, W., Nunez, M., 1975: Estimating global solar radiation. *Bound. Layer Meteor.,* **9**, 33–52.

Davis, J. C., 1986: *Statistics and Data Analysis in Geology* New York : John Wiley and Sons, 646 pp.

Haurwitz, B., 1945: Insolation in relation to cloudiness and cloud density. *J. Meteor.,* **2**, 154–166.

Haurwitz, B., 1948: Insolation in relation to cloud type. *J. Meteor.,* **5**, 110–113.

Huschke, R. E., 1969: Arctic Cloud Statistics from "Air-Calibrated" Surface Weather Observations. Memorandum, RM-6173-PR, The Rand Corporation.

Iqbal, M., 1983: An introduction to solar radiation. Toronto : Academic Press, 390 pp.

Kasten, F., Czeplak, G., 1980: Solar and terrestrial radiation dependent on the amount and type of cloud. *Solar Energy,* **24**, 177–189.

Martyn, D., 1992: *Climates of the World.* (Developments in Atmospheric Science 18). Amsterdam : Elsevier. 435 pp.

Meyers, T. P., Dale, R. F., 1983: Predicting daily insolation with hourly cloud height and coverage. *J. Climate Appl. Meteor.,* **22**, 537–545.

National Solar Radiation Data Base (1961–1990), 1992: User's Manual, Vol 1. Prepared by National Renewable Energy Laboratory.

Rossow, W. B., Zhang, Y.-C., 1995: Calculation of surface and top of atmosphere radiative fluxes from physical quantities based on ISCCP data sets. 2. Validation and first results. *J. Geophys. Res.,* **100**/D1, 1167–1197.

Schweiger, A. J., Key, J. R., 1992: Arctic cloudiness: comparison of ISCCP-C2 and Nimbus-7 Satellite-derived cloud products with a surface-based cloud climatology. *J. Climate,* **5,** 1514–1527.

Stone, R., Mefford, T., Dutton, E., Longenecker, D., Halter, B., Endres, D., 1996: Barrow, Alaska, Surface Radiation and Meteorological Measurements: January 1992 to December 1994. NOAA Data Report, ERL CMDL-11.

Norris, D. J., 1968: Correlation of solar radiation with clouds. *Solar Energy*, **12**, 107–112.

Suckling, P. W., Hay, J. E., 1997: A cloud layer-sunshine model for estimating direct, diffuse and total solar radiation. *Atmosphere,* **15**/4, 194–207.

Vowinckel, E., Orvig, S., 1962: Relation between solar radiation income and cloud type in the Arctic. *J. Appl. Meteor.,* **1**, 552–559.

Warren, S. G., Hahn, C. J., London, J., 1985: Simultaneous occurrences of different cloud types. *J. Climate Appl. Meteor.,* **24**, 658–667.

Wendler, G., 1983: Solar Radiation Data for Kodiak, Alaska. University of Alaska, Geophysical Institute Report, UAG R-299. 26 pp.

Wendler, G., Eaton, F., 1983: *Solar Radiation Data for Fairbanks. University of Alaska, Geophysical Institute Report. 58 pp.*

Wendler, G., Eaton, F., 1990: Surface radiation budget at Barrow, Alaska. *Theor. Appl. Climatol,* **41**, 107–115.

Wendler, G., Eaton, F. D., Ohtake, T., 1981: Multiple reflection effects on irradiance in the presence of arctic stratus clouds. *J. Geophys. Res.,* **86**/C3, 2049–2057.

Wendler, G., Kodama, Y., 1986: On the relationship between global radiation and cloudiness in Southern Alaska. *Solar Energy,* **36**, 431–435.

Wise, J. L., 1979: Alaska Solar Radiation Analysis. Arctic Environmental Information and Data Center, University of Alaska. Report for U. S. Department of Energy, 27 pp.

Authors' address: Dorte Dissing and Gerd Wendler, Alaska Climate Center, Geophysical Institute, University of Alaska Fairbanks, Fairbanks, AK 99775-0800, U.S.A. (e-mail: fsdd@aurora.alaska.edu)